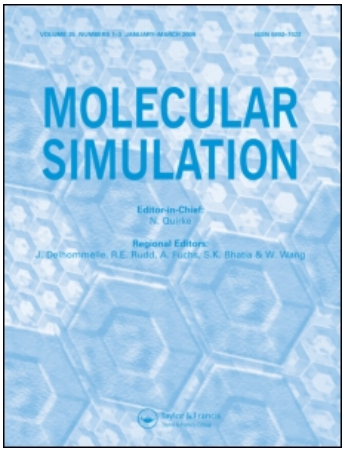


**Molecular Simulation**
Publication details, including instructions for authors and subscription information:
http://www.informaworld.com/smpp/title~content=t713644482

# Binding modes of protegrin-1, a beta-strand antimicrobial peptide, in lipid bilayers

S. K. Kandasamy[a]; R. G. Larson[a]
[a] Chemical Engineering Department, University of Michigan, Ann Arbor, MI, USA

**To cite this Article** Kandasamy, S. K. and Larson, R. G.(2007) 'Binding modes of protegrin-1, a beta-strand antimicrobial peptide, in lipid bilayers', Molecular Simulation, 33: 9, 799 — 807
**To link to this Article: DOI:** 10.1080/08927020701313737
**URL:** http://dx.doi.org/10.1080/08927020701313737

*Molecular Simulation*, Vol. 33, Nos. 9–10, 15–30 August 2007, 799–807

Taylor & Francis
Taylor & Francis Group

# Binding modes of protegrin-1, a beta-strand antimicrobial peptide, in lipid bilayers

S. K. KANDASAMY† and R. G. LARSON*

Chemical Engineering Department, University of Michigan, Ann Arbor, MI 48109, USA

*(Received December 2006; in final form March 2007)*

Molecular dynamics (MD) simulations of the interactions of a beta-strand antimicrobial peptide, protegrin-1, with model lipid bilayers of different hydrophobic widths show that protegrin-1 possesses at least two distinct binding modes in the trans-membrane orientation. In one of the modes, three of the cationic arginine residues bind to one bilayer leaflet and the other three arginine residues bind to the opposite leaflet, while in the second binding mode, four arginines bind to one leaflet and two to the other. The existence of multiple binding modes is facilitated by the high conformational flexibility of the first four residues of the N-terminal region, with a sequence of RGGR. One of the binding modes causes a larger bilayer disruption than the other, and in either mode, the bilayer disruption is smaller for lipid membranes with smaller bilayer widths. Simulations of the self-assembly of initially random lipid/water mixtures in the presence of PG-1 peptides show that the system evolves into a bilayer, with a stable water pore spanning the two lipid leaflets. Lipid head groups and the PG-1 peptide stabilize the water pore.

*Keywords*: Protegrin-1; Molecular dynamics simulations; Lipid bilayers; Beta sheet



## 1. Introduction

Antimicrobial peptides (AMP) are short, cationic peptides that interact with the lipid components of the cell membranes and form the front line of host defense against invading microorganisms [1]. In their membrane-associated state, AMPs typically acquire an amphipathic alpha-helical structure (e.g. magainins) or a beta-strand structure (e.g. protegrins, human defensins). While there is tremendous interest in AMPs as therapeutics, the exact mechanism of action of these peptides against the microbial target is yet unclear. It is still extremely challenging to apply experimental methods such as oriented circular dichroism [2–4], lamellar X-ray diffraction [5,6], neutron diffraction [7] and solid state NMR [8–15] techniques to understand the interactions of AMPs with lipid bilayers. Nevertheless, the topology, position, orientation and aggregation state of various alpha-helical and beta-strand AMPs in lipid bilayers have been determined [12–20].

Protegrin-1 (PG-1) is a broad-spectrum AMP, which is 18 residues long and is found in porcine leukocytes. It has six positively charged arginine residues and four cysteine residues. The sequence is NH2-RGGRLCYCRRRFCV-CVGR-CONH2. In solution, PG-1 forms an anti-parallel beta-strand, and the two strands are stabilized by two cysteine bridges formed among the four cysteine residues. This disulfide-stabilized beta-strand motif is frequently observed in other AMPs such as tachyplesin and human defensins. Over the past decade or so, several experimental studies have been undertaken to investigate the interactions of PG-1 peptides in model lipid bilayers [7,9–11,13,14,18]. At low peptide concentrations, PG-1 is typically bound to the head group region of the bilayer, at the lipid–water interface. At higher peptide concentrations, PG-1 is found to adopt a trans-membrane orientation. If the model lipid of the bilayer is relatively short (e.g. dilauryl-phosphatidyl-choline, DLPC, with 12 tail carbons) compared to the lipids of physiologically realistic membranes (e.g. palmitoyl-oleoylphosphatidyl-choline, POPC, with 18 and 16 tail carbons), the peptides adopt a transmembrane orientation without significantly affecting the overall membrane structure [9,13,19]. However, when the model lipid membrane has a hydrophobic width comparable to physiologically realistic membranes, significant membrane disruption

*Corresponding author. Tel.: + 1-734-936-0772. Fax: + 1-734-763-0459. Email: rlarson@umich.edu
†Email: senthilk@umich.edu

*Molecular Simulation*
ISSN 0892-7022 print/ISSN 1029-0435 online © 2007 Taylor & Francis
http://www.tandf.co.uk/journals
DOI: 10.1080/08927020701313737

and pore-formation is observed [13,19]. The pores thus formed seem to be lined with PG-1 aggregates [19].

Molecular dynamics (MD) simulations of peptide–lipid interactions have been valuable in providing structural information complementary to that provided by experimental techniques [20–31]. Solid state NMR, which is the method most commonly used to determine the structure of membrane associated peptides, is typically able to resolve the position and orientation of the peptide relative to the lipids, but, due to the fluid nature of the lipids surrounding the peptides, yields only a coarse, time-averaged depiction of the membrane structure. Atomistically specific interactions between the individual amino-acids of the peptides and the surrounding lipid molecules are difficult to resolve from these experimental studies. MD simulations are capable of determining these specific interactions and thus, in conjunction with experiments, provide a more complete picture of the lipid–peptide interactions. Several simulation studies have been undertaken over the years to investigate peptide–lipid interactions in general [21,22,24,28] and AMP-lipid interactions in particular [21,23,25–27,29–31]. Most of these simulations have focused on the alpha-helical class of AMPs such as magainins and its derivatives, ovispirins, etc. To date, very few studies have focused on beta-strand peptides such as protegrins [30,32,33].

The difference between PG-1, a beta-strand peptide, and alpha-helical peptides lies not only in the secondary structure, but also in the spatial distribution of charged residues. The cationic residues such as lysine and arginine are abundant in all AMPs and are thought to play a primary role in AMP activity. Most alpha-helical AMPs are amphipathic, with the charged and polar residues occupying one face of the helix and the hydrophobic residues occupying the other. This amphipathicity enables preferential partitioning of the peptides at the lipid/water (hydrophobic/hydrophilic) interface and promotes aggregation and pore formation under certain favorable conditions. PG-1, on the other hand, has six charged arginine (ARG) residues (figure 1), three of which (residues 9, 10 and 11) are in the turn region of the beta-strand, while the other three (residues 1, 4 and 18) are in the opposite, terminal, region of the strand. Thus, PG-1 is not a classic amphipathic peptide like most alpha-helical AMPs. Another significant feature of the PG-1 sequence is the presence of three glycine (GLY) residues at positions 2, 3 and 17, adjacent to the terminal ARG residues. Since the GLY residues provide larger flexibility to the peptide backbone, and because the ARG residues have long side chains which can sample large regions in space, the terminal region of the beta-strand is extraordinarily flexible (By "terminal" region, we refer to the N- and C-terminal region of the anti-parallel strand; i.e. residues 1 and 18. By the "turn" region, we refer to the opposite end of the strand; i.e. residues 9, 10 and 11). This aspect of the peptide structure should play an important role in its interactions with the lipid membranes. In this manuscript, we propose to investigate the role of the peptide flexibility

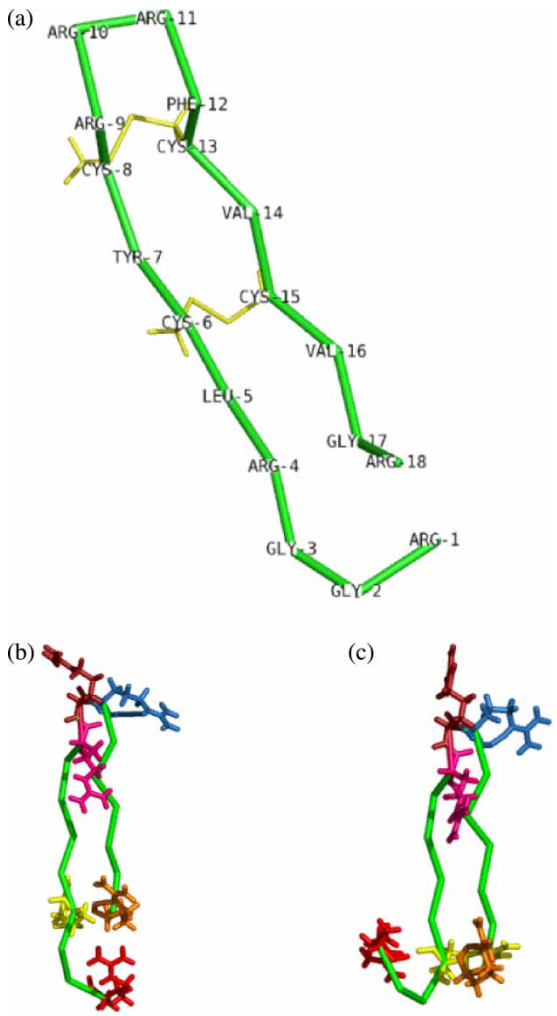


Figure 1. The structure of the protegrin-1 (PG-1) peptide. In part (a), the backbone trace is shown as green ribbons. The cysteine bridges are shown as yellow sticks. The sidechain atoms of the other residues are not shown. Part (b) shows the protegrin molecule in the PG1-OUT conformation and part (c) shows the protegrins molecule in the PG1-IN conformation. In parts (b) and (c), each ARG side chain is shown in different color.

and distribution of charged residues in interactions with lipid bilayers using MD simulations.

To date, only a small number of MD simulation studies have been performed on the interactions of PG-1 with lipid membranes [30,32,33]. Langham *et al.* [30] performed simulations of PG-1 with sodium-dodecyl-sulfate (SDS) and dodecyl-phospho-choline (DPC) micelles. These micelles were chosen to represent, respectively, the bacterial and mammalian membranes. They found that PG-1 has strong interactions with the head group regions of the micelles. Jang *et al.* [33] performed simulations of the interactions of PG-1 with more realistic model membrane bilayers consisting of either palmitoyl-oleoyl-phosphatidyl-choline (POPC) lipids to mimic mammalian membranes and mixed POPC/POPG lipids (where POPG stands for palmitoyl-oleoyl-phosphatidylglycerol, and is a negatively charged membrane lipid) to mimic bacterial membranes. They found that the peptides bind more strongly to the bacterial lipid mimic than

to the mammalian lipid mimic. In both aforementioned studies, a single PG-1 peptide was simulated with the model lipids. However, experiments have shown that PG-1 acts by forming pores in lipid bilayers that are supported by aggregates of multiple PG-1 peptides. Due to extremely high computational costs, it is currently difficult to simulate at an atomistic level multiple peptides interacting with lipid bilayers and obtain well equilibrate structures such as pores. In fact, to date, there has been only one long timescale simulation [34] that showed spontaneous pore formation in lipid bilayers using alpha-helical peptides. Experiments have shown that PG-1 facilitates pore formation only for large enough bilayer widths, corresponding to lipid tails that are at least 16 carbons long. Here, we probe the trans-membrane orientation of a single PG-1 in model lipid bilayers of different membrane widths, and determine the specific interactions between the different amino acids and the lipid bilayers and how these interactions are aided by peptide flexibility.

## 2. Methods

We used the GROMACS simulation program, version 3.2.1, for all of our simulations [35]. The coordinates of PG-1 were downloaded from the protein data bank (1PG1). The downloaded structure has 20 independent sets of PG-1 coordinates. We chose two of those coordinate sets for our simulations. In the first set of coordinates, the ARG residues on either end of the beta-strand are in the most extended conformations, stretching away from the peptide. We call this set of coordinates PG-1-OUT. A snapshot of this peptide, with all the ARG residues, is shown in figure 1(b). In the other set of coordinates, several ARG residues face "inward", towards the peptide center; we call this set of coordinates PG-1-IN. A snapshot of this peptide, with all the ARG residues, is shown in figure 1(c). Since we are interested in the effect of the flexibility of PG-1 peptide on its interactions with lipids, we chose these two sets of initial coordinates because they represent extremes in the range of possible initial conditions. Four different lipid bilayers, with different hydrophobic widths, were used. The lipids used were dilauryl-phosphatidyl-choline (DLPC, 12 carbons per tail), dimyristoyl-phosphatidylcholine (DMPC, 14 carbons per tail), dipalmitoyl-phosphatidyl-choline (DPPC, 16 carbons per tail) and palmitoyl-oleoyl-phosphatidyl-choline (POPC, 16 in one tail and 18 carbons in the other). The coordinates for the different bilayers were obtained from long, well-equilibrated simulations performed in our lab, using initial bilayer coordinates from the website of Peter Tieleman (http://moose.bio.ucalgary.ca). All bilayers consisted of 128 lipid molecules (64 per leaflet) and $\sim$5000 water molecules.

In each of the simulations, a single peptide was inserted into the lipid bilayer using the "hole" method of Faraldo-Gomez *et al.* [36]. Peptides having each of the two sets of peptide coordinates (PG-1-OUT and PG-1-IN) were inserted into each of the four lipid bilayers (DLPC, DMPC, DPPC and POPC) with two different initial peptide tilt angles (0° and 45° relative to the bilayer normal), thus giving us 16 different initial coordinates. In the insertion protocol, the $z$ coordinate of the center of mass of the peptide was set to that of the center of mass of the lipids, so that each peptide was inserted roughly in the middle of the bilayer. For each of these 16 sets of coordinates, a short equilibration period of 1 ns preceded the production run, during which the peptide backbone atoms were constrained. Then, the constraints were released and the systems were simulated for at least 30 ns each. Some of the simulations were extended to 50 ns and a few others to 100 ns. The simulations were performed in an NPT ensemble. The system was coupled to a Berendsen thermostat at 303 K for DLPC lipids, at 310 K for DMPC and POPC lipids, and at 323 K for DPPC lipids. All systems were coupled to a Berendsen barostat at 1 atm pressure. The pressure coupling was semiisotropic, with the lateral and normal directions coupled separately. A time step of 2 fs was used and all bonds were constrained using the LINCS algorithm [37]. Van der Waals and short-range electrostatic interactions were cut-off at 1.2 nm. Long range electrostatic interactions were calculated using the particle mesh Ewald summation technique [38]. Coordinates were saved every pico-second and were used in subsequent analysis. The simulations are listed in table 1.

## 3. Results and discussion

### 3.1 Peptide orientation and binding

The final peptide orientation and the nature of the specific interactions between the lipids and the amino acids are

Table 1. List of simulations and their durations.

| *Peptides* | *Lipids* | | | |
|---|---|---|---|---|
| | *DLPC* | *DMPC* | *DPPC* | *POPC* |
| PG-1-IN (0°) | Sim1–100 ns | Sim5–50 ns | Sim9–100 ns | Sim13–100 ns |
| PG-1-IN (45°) | Sim2–100 ns | Sim6–50 ns | Sim10–100 ns | Sim14–100 ns |
| PG-1-OUT (0°) | Sim3–30 ns | Sim7–30 ns | Sim11–30 ns | Sim15–30 ns |
| PG-1-OUT (45°) | Sim4–30 ns | Sim8–30 ns | Sim12–30 ns | Sim16–30 ns |

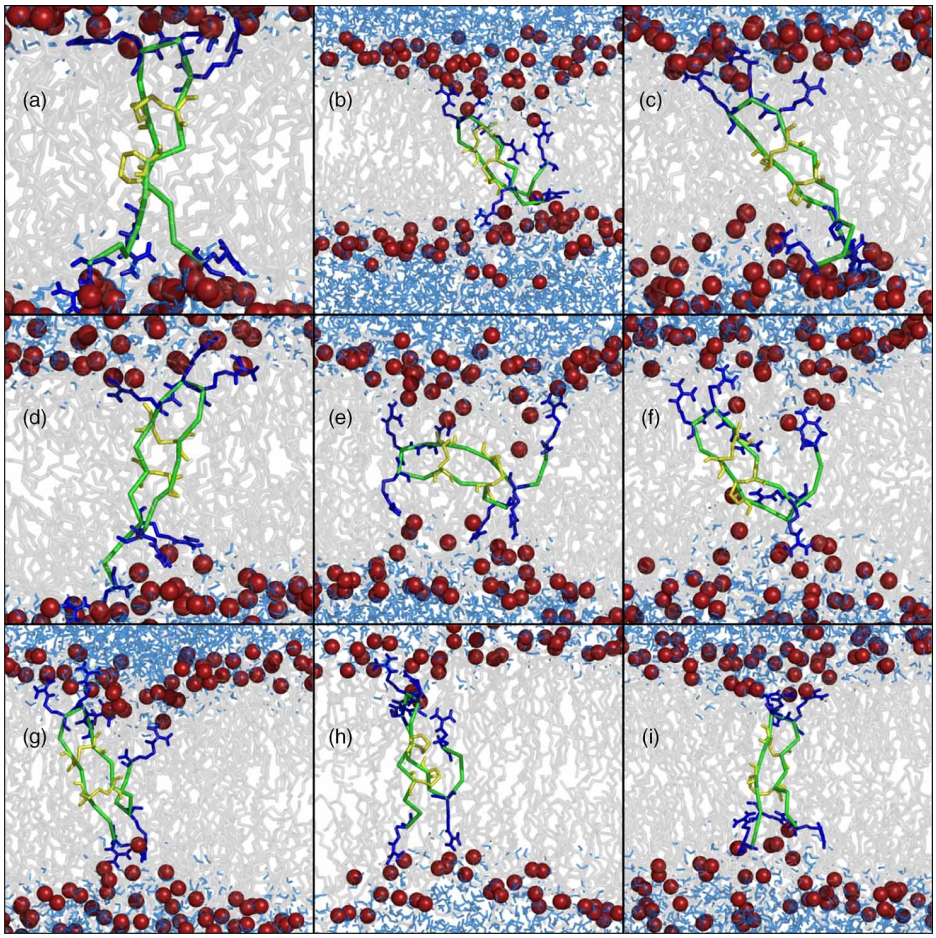


Figure 2. Snapshots at the end of several simulations. In all the subfigures, the PG-1 peptide is shown as a green ribbon. The cysteine bridge is shown as yellow sticks and the arginine residues are shown as blue sticks. The lipid phosphorus atoms are shown as red spheres, the lipid molecules as grey sticks and water molecules as light-blue sticks. Parts (a), (b) and (c) contain DLPC bilayers, while (d), (e) and (f) contain POPC bilayers, and (g), (h) and (i) contain DPPC bilayers. For a given bilayer, the various simulations were started with different initial conditions of the peptide (colour in online version).



strongly dependent on the initial conditions. The snapshots from the end of nine of the simulations are shown in figure 2; three from DLPC bilayers, (a, b and c), three from POPC bilayers (d, e and f), and three from DPPC bilayers (g, h and i). The most striking observation is the position of the different ARG residues relative to the two bilayer leaflets. In figure 2(a),(c),(d),(i), the three terminal-ARG residues (ARG1, ARG4 and ARG18) interact with one of the lipid leaflets while the three turn-ARG residues (ARG9, ARG10 and ARG11) interact with the opposite lipid leaflet. In all of these simulations, the peptide was initially in the PG-1-OUT conformation, with the ARG residues extended outward. Thus, after insertion into the bilayer, either in the vertical or 45° initial orientation, the ARG residues were already close to the lipid leaflets and then during the coarse of the simulation, bind strongly to the lipid leaflet closest to them. However, most peptides that start in the PG-1-IN conformation have their ARG residues closer to the bilayer center, than do the PG-1-OUT peptides. During the initial equilibration period, when the peptide backbone is constrained, the lipid molecules adapt their conformations to the peptide, to form favorable interactions with the ARG residues, which are energetically disfavored in the hydrophobic lipid tail region. Once the constraints are released, the peptide-lipid system re-adapts during the coarse of the simulation. We find that for the PG-1-IN initial conditions, some of the final configurations are similar to that of PG-1-OUT final configurations; i.e. ARG1, ARG4 and ARG18 interact with one leaflet of the bilayer, while ARG9, ARG10 and ARG11 interact with the other leaflet. However, most of the PG-1-IN initial conditions lead to a configuration where one of the terminal ARG residues, ARG1, interacts with the same leaflet of the bilayer as do ARG9, ARG10 and ARG11, while ARG 4 and ARG18 interact with the other leaflet. This is evident from figure 2(b),(f)–(h). Fifteen of the sixteen simulations show one of these two binding modes; i.e. ARG9-ARG10-ARG11-leaflet1/ARG1-ARG4-ARG18-leaflet2 (which we will refer to as binding-mode-1, 8 instances) or ARG1-ARG9-ARG10-ARG11-leaflet1/ARG4-ARG18-leaflet2 (binding-mode-2, 7 instances). In one rare case (figure 2(e)), ARG1, ARG9 and ARG10 bind to one leaflet while ARG4, ARG11 and ARG18 bind to the other leaflet. The binding mode at the end of the simulations is listed in table 2.

Table 2. Binding modes for each of the simulations.

| | *Lipid* | *Initial peptide configuration* | *Initial peptide orientation (°)* | *Binding mode* |
|---|---|---|---|---|
| 1 | DLPC | IN | 0 | 2 |
| 2 | DLPC | IN | 45 | 2 |
| 3 | DLPC | OUT | 0 | 1 |
| 4 | DLPC | OUT | 45 | 1 |
| 5 | DMPC | IN | 0 | 1 |
| 6 | DMPC | IN | 45 | 2 |
| 7 | DMPC | OUT | 0 | 1 |
| 8 | DMPC | OUT | 45 | 2 |
| 9 | DPPC | IN | 0 | 2 |
| 10 | DPPC | IN | 45 | 1 |
| 11 | DPPC | OUT | 0 | 2 |
| 12 | DPPC | OUT | 45 | 1 |
| 13 | POPC | IN | 0 | 1 |
| 14 | POPC | IN | 45 | 3 |
| 15 | POPC | OUT | 0 | 2 |
| 16 | POPC | OUT | 45 | 1 |

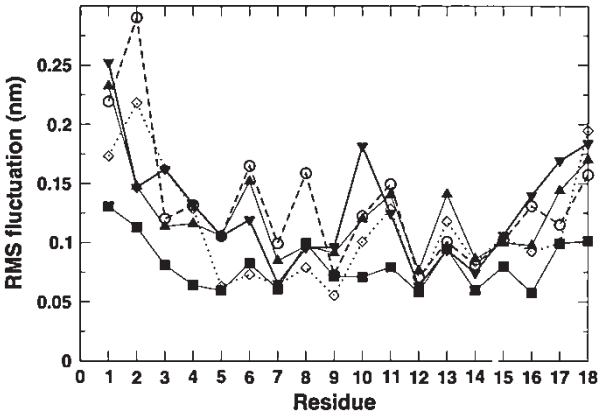


Figure 4. The root mean square fluctutations of the peptide from five representative simulations. Largest fluctuations are seen for the terminal residues.

### *3.2 Flexible RGGR domain*

In our simulations, binding-mode-2 occurs almost as often as binding-mode-1. This is presumably due to the extraordinary flexibility of the first four residues of the peptide (RGGR domain), whereas residues 6–15 are highly constrained due to the double cysteine bridges. The high flexibility is due to the high probability of dihedral transitions, leading to larger rotomeric configurational sampling. In figure 3, we show the number of rotameric transitions (simply, the back bone dihedral transitions) as a function of residue number of the peptide for a representative simulation (Sim1 in table 1). Clearly, the N- and C-terminal regions show a high number of dihedral transitions, with the RGGR domain showing the largest number. This is also evident from the root mean square fluctuations of the residues from five representative simulations (figure 4). The first three residues near the N-terminus show the largest fluctuations. This large conformational flexibility enables ARG1 to participate in two distinct binding modes.

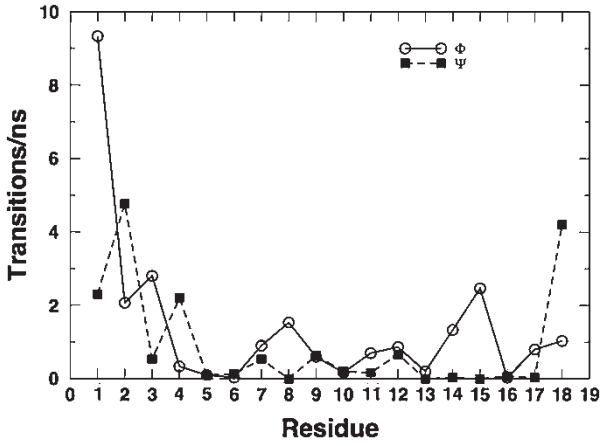


Figure 3. The number of rotamer transitions per nanosecond (transitions of $\phi$ and $\psi$ dihedral angles) as a function of residue number for PG-1 for a representative simulation. The most frequent transitions occur for residues 1–3 and residue 18.

### *3.3 Bilayer disruption*

On average, we find that bilayer disruption is smaller for binding-mode-1 than for binding-mode-2. This is not surprising, since the peptide is better able to span the hydrophobic width of the bilayer in binding-mode-1 than in binding-mode-2. The peptide is able to fully span the DLPC (thinnest) bilayer without significantly disrupting the lipids in binding-mode-1 (figure 2(a)), and produce only minor disruption in binding-mode-2 (figure 2(b).) However, for the much thicker POPC or DPPC bilayers, even in binding-mode-1, lipid disruption is observed, which becomes even greater in binding-mode-2. The disruption largely involves the peptide pulling several lipid molecules towards the bilayer center, effectively reducing the hydrophobic width of the bilayer. We approximated the extent of bilayer disruption in the two different binding modes by calculating the shrinkage of the bilayer relative to the corresponding peptide-free bilayer. The shrinkage was defined as the difference between the bilayer width (average phosphorus-phosphorus distance between the two lipid leaflets) of a peptide-free membrane and the bilayer width of the peptide-bound membrane. The bilayer widths for the peptide-free membranes were calculated from long simulations of DLPC, DPPC, DMPC and POPC bilayers from earlier work [28,29]. For the peptide-bound bilayers, the average bilayer width was calculated from the latter half of the simulation. We show the results from all 16 simulations in figure 5. It is clear that binding-mode-2 disrupts the bilayer to a larger extent than does binding-mode-2. We also find that on an average, the bilayers with larger hydrophobic widths show larger disruption, presumably to achieve better hydrophobic matching.

Even in binding-mode-2, the shrinkage can be relatively small under certain circumstances. In figure 2(h), in DPPC bilayers, ARG1 and ARG4 are bound to the opposite leaflets. Yet the bilayer shrinkage is relatively minimal ($\sim$0.5 Å) in this case. This is because the ARG1 and ARG4 residues are fully extended in opposite directions.

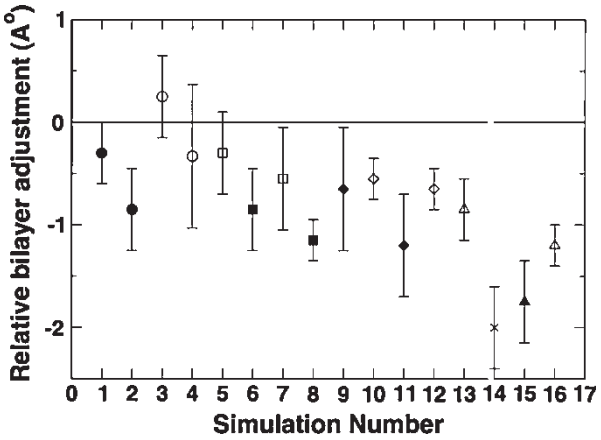


Figure 5. Relative bilayer shrinkage for all 16 simulations. On average, for the simulations where binding-mode-1 is observed (open symbols), the bilayer disruptions are smaller than those where binding-mode-2 is observed (closed symbols). DLPC simulations are shown as circles (○), DMPC bilayers as squares (□), DPPC bilayers as diamonds (◇) and POPC bilayers as triangles (△). The star refers to binding mode 3. The simulation number on the abscissa corresponds to those from table 2.

In figure 6, we show the distance between the center of mass of the three nitrogen atoms in each of the side chains of ARG1 and ARG4. Under almost fully extended conditions, the inter-arginine distance can reach nearly 25 Å. In most cases of binding-mode-1, the distance is typically 6 Å or so. This further corroborates the large conformational flexibility of the RGGR motif.

### 3.4 Peptide–lipid interaction energy

The two dominant binding modes seem to appear at roughly equal frequencies in our simulations but are highly dependent on the initial conditions. It is extremely difficult to estimate the free energy difference between the two states, due to inadequate sampling in the limited timescales of the simulation. However, it is possible to calculate the dominant interactions between the peptides and the lipids.

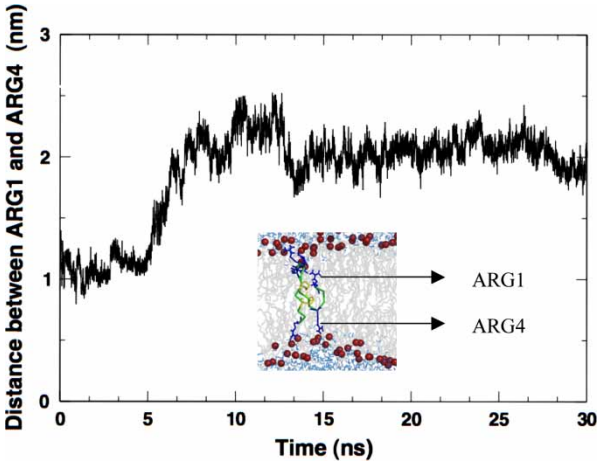


Figure 6. The distance between the ARG1 and ARG4 residues of a simulation in binding-mode-2. A separation as large as 24 Å is observed for this particular simulation. The inset shows the final snapshot from the simulation.

We calculated the Lennard–Jones and Coulomb interactions between different sections of the lipids and the various amino acids of the peptide. The largest contributions for the interaction energies were from the Coulomb interactions between the ARG residues and the charged regions of the lipids. Interestingly, ARG residues at different depths along the lipid bilayer had nearly the same Coulomb interaction energies. This is realized by different strengths of interaction with the glycerol and phosphate moieties of the lipid bilayers. In figure 7, we show a typical case, where the Coulomb interactions between two ARG residues from a representative simulation (Sim13, table 1) are shown (figure 7(a),(b)). ARG11, which is bound deeply into the lipid–water interface, interacts strongly with the phosphate region of the lipids, while ARG18, which is less deeply bound, interacts strongly with the glycerol region of the lipids. In figure 7(c), the total Coulomb interaction energies for the two ARG residues are shown. The magnitudes are approximately the same for both the ARG residues, at ~150 kJ/mol. We find this to be true for most ARG residues from most of the simulations. The lipids adapt their configurations to the ARG residues to provide favorable electrostatic interactions, either through the glycerol or the phosphate regions. The Lennard–Jones interaction energies follow a similar trend, with nearly matching values for all peptide–lipid combinations.

### 3.5 Insights from self-assembly

In all the cases listed in table 1, the PG-1 peptide was initially inserted into a preformed bilayer in a transmembrane orientation and the subsequent simulation revealed possible interactions between the peptides and lipids. The results from these simulations largely confirm experimental observations, while providing additional details about specific molecular features, such as the different binding modes. Experiments show that PG-1 induces pores in POPC bilayers [3,10,11,19] while it does not induce pores in thinner DLPC bilayers. Our simulations show that the POPC bilayers are disrupted to a larger extend than DLPC bilayers. However, pore formation is not observed in our simulations, because this requires multiple peptides and larger system sizes and our simulation setup lacks these driving forces necessary to induce pores.

Hydrophilic pores are formed during simulations of the spontaneous self-assembly of random lipid–water mixtures [39]. These pores are stable for timescales of tens of nano-seconds, but eventually collapse, to yield fully healed lipid bilayers. If a stabilizing agent, such as an AMP were lining the pore, then the pore would presumably be stable for longer timescales. Simulation studies of such a pore would provide insights into the interactions between the lipids, the water molecules and the peptides, which can help understand the structure of pores formed by AMP aggregates. In principle, one should be able to generate a pore lined with AMPs by means

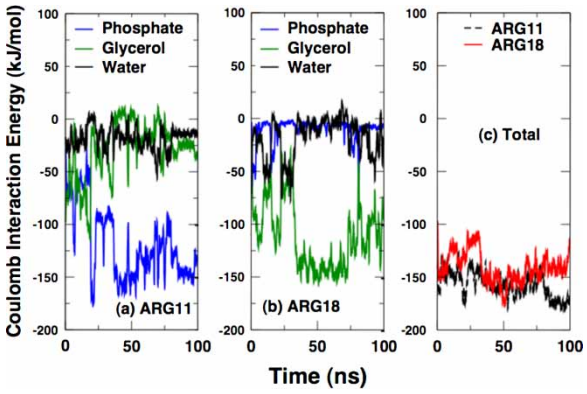


Figure 7. Coulomb interaction energies between different moieties of the lipid bilayer and (a) ARG11 (b) ARG18 in a representative simulation. (c). The total Coulomb interaction energy for the two residues.

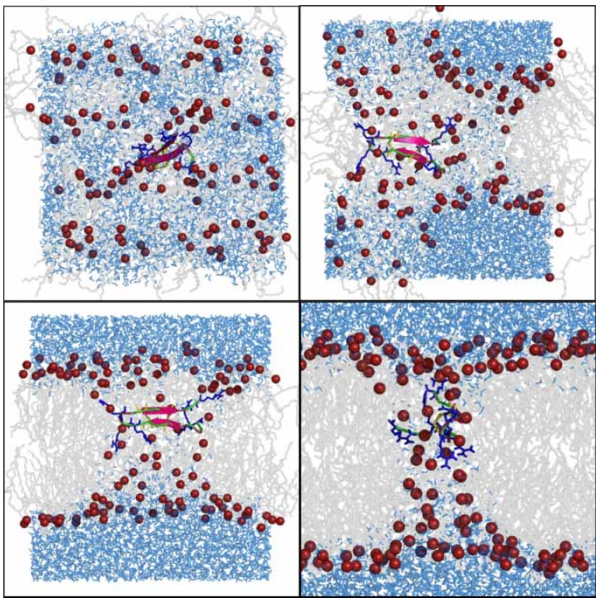

Figure 8. Snapshots during the self-assembly of a random POPC/water/PG-1 mixture. Top-left, initial condition; top-right, at 50 ns; bottom-left, at 100 ns; bottom-right, at 200 ns. The peptide is shown as a green and pink cartoon. The ARG residues are shown in blue and the cysteine bridge is shown in yellow. Water molecules are shown in light-blue, lipid molecules as grey sticks, and lipid phosphorus atoms as red spheres. The final snapshot shows a water pore, spanning the bilayer, stabilized by the lipid headgroups and the PG-1 peptide (colour in online version).

of spontaneous self-assembly from a random initial state that contains enough lipids and peptides. However, such a simulation would require extremely large system sizes and is not possible to perform at the present time. A compromise is to simulate a single peptide with a random lipid mixture. While this may not provide a complete picture of the pores induced by AMPs, it nevertheless provides a slice of information about peptide–pore interactions.

To test this hypothesis, we performed several long simulations of single PG-1 molecules in random mixtures of lipids and water. 128 lipids were randomly placed in a cubic box of size 6.5 × 6.5 × 6.5 nm. Then the box was solvated with water. A single PG-1 molecule was placed with a random orientation at the middle of the box. This system, corresponding to an arbitrarily large temperature, was suddenly "quenched" to 310 K. Each simulation was performed in the NPT ensemble, with the system coupled to a Berendsen thermostat at 310 K and a Berendsen barostat at 1 atm pressure. For the first 20 ns of the simulations, the pressure was coupled isotropically in all three dimensions (i.e. the box remained cubic). After 20 ns, anisotropic pressure coupling was applied, to promote the system to evolve into its preferred phase. The initial isotropic coupling period is necessitated by the small system size and the tendency of the simulation cell to shrink quickly in one linear dimension if coupled anisotropically. Van der Waals and Coulomb interactions used a short-range cut-off of 1.2 nm. The long range electrostatic interactions were calculated using the particle mesh Ewald method.

We performed several such simulations with POPC membranes for up to 200 ns each. The results from the various simulations were essentially similar and we show the snapshots from one such simulation in figure 8. Snapshots at the beginning (top-left), at 50 ns (top-right), at 100 ns (bottom-left) and at 200 ns (bottom-right) are shown. Initially, the lipids are in a random state. Soon, large hydrophobic nuclei, comprised of lipid tails, begin to form (50 ns). At 100 ns, a pseudo-bilayer, with large water pore is formed. This water pore continues to exist through the duration of the simulation, stabilized by the PG-1 peptide. Over similar timescales, peptide-free quenching simulations always formed defect free bilayers [39]. The pore region contains water molecules, lined by the lipid head groups. There are strong hydrogen bonding interactions between the ARG residues of the PG-1 peptide and the lipid head groups, which keeps the pore stable, at least over the simulation timescale. The number of hydrogen bonds formed between the peptide and the lipids at the end of the quenching simulation is smaller than those between the peptide and the lipids in a pore-free trans-membrane simulation (simulations 13–16, table 1.) However, when the number of water–peptide hydrogen bonds is taken into account, the total number of hydrogen bonds formed by the peptides is almost identical for the quenched and trans-membrane peptides. The peptide does not take on a trans-membrane orientation at the end the quenching simulations. However, at this moment, it is not possible for us to comment on the preferred orientation of the pore-associate peptide due to insufficient statistics. With larger systems, presumably, several such peptide-stabilized pores could form, which with sufficient time (at least microseconds) could aggregate to form a true "toroidal" like pore as observed in experiments. Nevertheless, the self-assembly simulations at least suggest that the pores can be stabilized by the PG-1 peptides.

While most of our trans-membrane simulations yielded final configurations corresponding to one of two binding modes, we must allow for the possibility of other, less common binding configurations such as that shown in figure 2(e), especially if other peptide initial conditions are

chosen (different initial side chain orientations, different overall peptide tilt relative to the bilayer normal). Such configurations may promote larger bilayer disruption and may play a vital role in the insertion and pore-formation mechanism of PG-1 aggregates. However, from the set of initial conditions employed in our study, we observe only two dominant binding modes. The high conformational flexibility of the first four residues (RGGR) clearly makes multiple binding conformations feasible. However, the exact implications of this conformational flexibility are not evident from our simple simulations. Nevertheless, it should be noted that the minimum inhibitory concentrations (MIC) required to kill microbes increases by an order of magnitude when the first four amino acids (RGGR) are removed from the PG-1 sequence [40], suggesting an important role for these residues in membrane binding, pore formation and antimicrobial activity.

Recent solid-state NMR studies suggest that the pores formed by the PG-1 aggregates are extremely ordered, with well-defined multiples of parallel-dimers lining the pores. It is not currently possible to reproduce these experimental structures using all-atom MD simulations. It is also worth mentioning that while alphahelical peptides such as magainins have traditionally been thought to form well-ordered toroidal pores, recent simulations suggest that the pores may in fact be disordered [34].



## 4. Conclusions

Our systematic simulations of the beta-strand AMP protegrin-1 in various model lipid bilayers show that in the trans-membrane state, the peptide exhibits two prominent binding modes. In one of the modes, the three N-terminal arginine residues are hydrogen bonded to one leaflet of the bilayer, while the three turn arginines are hydrogen bonded to the other leaflet. In the other mode, four arginines are bonded to one leaflet and two to the other. The first four residues of the N-terminal region show extraordinary conformational flexibility, which facilitate the two binding modes. The ARG1 residue, in particular, is able to sample large regions in space, making it possible to bind to either leaflet of the lipid bilayer. The second binding mode causes larger bilayer disruption than the other. We also find that the bilayer disruption is larger for lipids with larger hydrophobic widths. This is due to local lipid adaptations to minimize unfavorable interactions. The larger bilayer disruptions presumably make pore formation easier and this explains why PG-1 induces pores in thicker POPC bilayers and not in thinner DLPC bilayers. Simulations of the spontaneous self-assembly of random lipid mixtures in the presence of PG-1 lipids show that the final structure, which is stable at least in the simulation timescale of 200 ns, is a bilayer with a water pore spanning the two leaflets, with the pore stabilized by the PG-1 peptide. Our simulation study provides insights into the molecular events that occur during peptide–lipid interactions and pore formation. Currently, it is not possible to simulate systems large enough to study larger aggregates of peptides. Nevertheless, improving computational capabilities and combination of coarse-grained and atomistic simulations can provide information that is valuable and complementary to those obtained from experiments.

## References


[1] M. Zasloff. Antimicrobial peptides of multicellular organisms. *Nature*, **415**, 389 (2002).

[2] S.J. Ludtke, K. He, Y. Wu, H.W. Huang. Cooperative membrane insertion of magainin correlated with its cytolytic activity. *Biochim. Biophys. Acta*, **1190**, 181 (1994).

[3] W.T. Heller, A.J. Waring, R.I. Lehrer, H.W. Huang. Multiple states of beta-sheet peptide protegrin in lipid bilayers. *Biochemistry*, **37**, 17331 (1998).

[4] A. Ramamoorthy, S. Thennarasu, D.K. Lee, A. Tan, L. Maloy. Solid-state NMR investigation of the membrane-disrupting mechanism of antimicrobial peptides MSI-78 and MSI-594 derived from magainin 2 and melittin. *Biophys. J.*, **91**, 206 (2006).

[5] F.Y. Chen, M.T. Lee, H.W. Huang. Evidence for membrane thinning effect as the mechanism for peptide-induced pore formation. *Biophys. J.*, **84**, 3751 (2003).

[6] C. Li, T. Salditt. Structure of magainin and alamethicin in model membranes studied by X-ray reflectivity. *Biophys. J.*, **91**, 3285 (2006).

[7] L. Yang, T.M. Weiss, R.I. Lehrer, H.W. Huang. Crystallization of antimicrobial pores in membranes: magainin and protegrin. *Biophys. J.*, **79**, 2002 (2000).

[8] F.M. Marassi, S.J. Opella. A solid-state NMR index of helical membrane protein structure and topology. *J. Magn. Reson.*, **144**, 150 (2000).

[9] J.J. Buffy, T. Hong, S. Yamaguchi, A.J. Waring, R.I. Lehrer, M. Hong. Solid-state NMR investigation of the depth of insertion of protegrin-1 in lipid bilayers using paramagnetic Mn2 + . *Biophys. J.*, **85**, 2363 (2003).

[10] J.J. Buffy, A.J. Waring, R.I. Lehrer, M. Hong. Immobilization and aggregation of the antimicrobial peptide protegrin-1 in lipid bilayers investigated by solid-state NMR. *Biochemistry*, **42**, 13725 (2003).

[11] R. Mani, J.J. Buffy, A.J. Waring, R.I. Lehrer, M. Hong. Solid-state NMR investigation of the selective disruption of lipid membranes by protegrin-1. *Biochemistry*, **43**, 13839 (2004).

[12] J.X. Lu, K. Damodaran, J. Blazyk, G.A. Lorigan. Solid-state nuclear magnetic resonance relaxation studies of the interaction mechanism of antimicrobial peptides with phospholipid bilayer membranes. *Biochemistry*, **44**, 10208 (2005).

[13] R. Mani, A.J. Waring, R.I. Lehrer, M. Hong. Membrane-disruptive abilities of betahairpin antimicrobial peptides correlate with conformation and activity: a 31P and 1H NMR study. *Biochim. Biophys. Acta*, **1716**, 11 (2005).

[14] M. Tang, A.J. Waring, M. Hong. Intermolecular packing and alignment in an ordered beta-hairpin antimicrobial peptide aggregate from 2D solid-state NMR. *J. Am. Chem. Soc.*, **127**, 13919 (2005).

[15] E. Strandberg, P. Wadhwani, P. Tremouilhac, U.H. Durr, A.S. Ulrich. Solid-state NMR analysis of the PGLa peptide orientation in DMPC bilayers: structural fidelity of 2Hlabels versus high sensitivity of 19F-NMR. *Biophys. J.*, **90**, 1676 (2006).

[16] M. Tang, A.J. Waring, R.I. Lehrer, M. Hong. Orientation of a beta-hairpin antimicrobial peptide in lipid bilayers from two-dimensional dipolar chemical-shift correlation NMR. *Biophys. J.*, **90**, 3616 (2006).

[17] T. Doherty, A.J. Waring, M. Hong. Peptide–lipid interactions of the beta-hairpin antimicrobial peptide tachyplesin and its linear derivatives from solid-state NMR. *Biochim. Biophys. Acta*, **1758**, 1285 (2006).

[18] R. Mani, M. Tang, X. Wu, J.J. Buffy, A.J. Waring, M.A. Sherman, M. Hong. Membrane-bound dimer structure of a beta-hairpin antimicrobial peptide from rotationalecho double-resonance solid-state NMR. *Biochemistry*, **45**, 8341 (2006).

[19] R. Mani, S.D. Cady, M. Tang, A.J. Waring, R.I. Lehrer, M. Hong. Membrane dependent oligomeric structure and pore formation of a beta-hairpin antimicrobial peptide in lipid bilayers from solid-state NMR. *Proc. Natl. Acad. Sci. USA*, **103**, 16242 (2006).

[20] T. Doherty, A.J. Waring, M. Hong. Membrane-bound conformation and topology of the antimicrobial peptide tachyplesin I by solid-state NMR. *Biochemistry*, **45**, 1332 (2006).

[21] D.P. Tieleman, H.J. Berendsen, M.S. Sansom. Voltage-dependent insertion of alamethicin at phospholipid/water and octane/water interfaces. *Biophys. J.*, **80**, 331 (2001).

[22] B. Roux. Computational studies of the gramicidin channel. *Acc. Chem. Res.*, **35**, 366 (2002).

[23] C.M. Shepherd, H.J. Vogel, D.P. Tieleman. Interactions of the designed antimicrobial peptide MB21 and truncated dermaseptin S3 with lipid bilayers: molecular-dynamics simulations. *Biochem. J.*, **370**, 233 (2003).

[24] M.P. Aliste, J.L. MacCallum, D.P. Tieleman. Molecular dynamics simulations of pentapeptides at interfaces: salt bridge and cation–pi interactions. *Biochemistry*, **42**, 8976 (2003).

[25] S.K. Kandasamy, R.G. Larson. Binding and insertion of alpha-helical anti-microbial peptides in POPC bilayers studied by molecular dynamics simulations. *Chem. Phys. Lipids*, **132**, 113 (2004).

[26] H. Khandelia, Y.N. Kaznessis. Molecular dynamics simulations of helical antimicrobial peptides in SDS micelles: what do point mutations achieve? *Peptides*, **26**, 2037 (2005).

[27] C. Appelt, F. Eisenmenger, R. Kuhne, P. Schmieder, J.A. Soderhall. Interaction of the antimicrobial peptide cyclo(RRWWRF) with membranes by molecular dynamics simulations. *Biophys. J.*, **89**, 2296 (2005).

[28] S.K. Kandasamy, R.G. Larson. Molecular dynamics simulations of model trans-membrane peptides in lipid bilayers: a systematic investigation of hydrophobic mismatch. *Biophys. J.*, **90**, 2326 (2006).

[29] S.K. Kandasamy, R.G. Larson. Effect of salt on the interactions of antimicrobial peptides with zwitterionic lipid bilayers. *Biochim. Biophys. Acta*, **1758**, 1274 (2006).

[30] A.A. Langham, H. Khandelia, Y.N. Kaznessis. How can a beta-sheet peptide be both a potent antimicrobial and harmfully toxic? Molecular dynamics simulations of protegrin-1 in micelles. *Biopolymers*, **84**, 219 (2006).

[31] P. La Rocca, P.C. Biggin, D.P. Tieleman, M.S. Sansom. Simulation studies of the interaction of antimicrobial peptides and lipid bilayers. *Biochim. Biophys. Acta*, **1462**, 185 (1999).

[32] H. Khandelia, A.A. Langham, Y.N. Kaznessis. Driving engineering of novel antimicrobial peptides from simulations of peptide–micelle interactions. *Biochim. Biophys. Acta*, **1758**, 1224 (2006).

[33] H. Jang, B. Ma, T.B. Woolf, R. Nussinov. Interaction of protegrin-1 with lipid bilayers: membrane thinning effect. *Biophys. J.*, **91**, 2848 (2006).

[34] H. Leontiadou, A.E. Mark, S.J. Marrink. Antimicrobial peptides in action. *J. Am. Chem. Soc.*, **128**, 12156 (2006).

[35] D. Van Der Spoel, E. Lindahl, B. Hess, G. Groenhof, A.E. Mark, H.J. Berendsen. GROMACS: fast, flexible, and free. *J. Comput. Chem.*, **26**, 1701 (2005).

[36] J.D. Faraldo-Gomez, G.R. Smith, M.S. Sansom. Setting up and optimization of membrane protein simulations. *Eur. Biophys. J.*, **31**, 217 (2002).

[37] B. Hess, H. Bekker, H.J.C. Berendsen, J.G.E.M. Fraaije. LINCS: a linear constraint solver for molecular simulations. *J. Comp. Chem.*, **18**, 1463 (1997).

[38] U. Essmann, L. Perera, L. Berkowitz. A smooth particle mesh Ewald method. *J. Chem. Phys.*, **103**, 8577 (1995).

[39] S.J. Marrink, E. Lindahl, O. Edholm, A.E. Mark. Simulation of the spontaneous aggregation of phospholipids into bilayers. *J. Am. Chem. Soc.*, **123**, 8638 (2001).

[40] N. Ostberg, Y. Kaznessis. Protegrin structure–activity relationships: using homology models of synthetic sequences to determine structural characteristics important for activity. *Peptides*, **26**, 197 (2005).